Antiferromagnetism, Ferromagnetism, and Phase Separation in the GMR System $Sr_{2-x}La_{1+x}Mn_2O_7$

P. D. Battle,*,† D. E. Cox,‡ M. A. Green,† J. E. Millburn,† L. E. Spring,† P. G. Radaelli,§ M. J. Rosseinsky,*,† and J. F. Vente†

Inorganic Chemistry Laboratory, University of Oxford, South Parks Road, Oxford OX1 3QR, U.K.; Department of Physics, Brookhaven National Laboratory, Upton, New York 11973; and Institut Laue-Langevin, BP 156X, 38042 Grenoble Cedex 9, France

Received December 13, 1996. Revised Manuscript Received February 3, 1997⊗

Neutron and synchrotron X-ray powder diffraction techniques have been used to refine the crystal and magnetic structures of the $n = 2$ Ruddlesden−Popper (RP) system $Sr_2LaMn_2O_7$. The sample is shown to be biphasic, although both phases are of the RP type and have similar structural parameters. The majority phase (81%) adopts a collinear antiferromagnetic structure below ∼210 K whereas the minority phase is ferromagnetically ordered below ∼125 K. The ordered magnetic moments lie in the *xy* plane in both phases. The behavior observed is discussed in terms of the interplay between structural and electronic factors. Comparison with data obtained previously by other workers leads to the conclusion that our results have some general significance in the study of $n = 2$ RP systems.

Introduction

The observation of giant magnetoresistance (GMR) just above the Curie temperatures (T_c) of the pseudocubic perovskites $Ln_{1-x}A_xMnO_3$ (Ln = lanthanide, Bi; A = Ca, Ba, Sr, Pb) has attracted considerable attention.[1−5] All of these manganates have an insulating, high-temperature paramagnetic phase and a metallic, low-temperature phase which shows a spontaneous magnetization. The coexistence of metallic conductivity and ferromagnetic coupling at low temperatures has been accounted for in terms of a double exchange (DE) process[6,7] which requires the presence of a mixed valence state with a nonintegral number of d-electrons per Mn cation. The observed magnetoresistance is then explained by assuming that the additional spin alignment caused by the external field effectively moves the metal−insulator transition to $T > T_c$. Recently, GMR has been discovered in compounds that apparently do not fulfill the requirements of this model. $Tl_2Mn_2O_7$, for example, becomes ferromagnetic and shows a field-dependent resistivity around the Curie temperature (142 K),[8−10] but all the Mn appears to be tetravalent and the GMR therefore cannot readily be explained using a simple DE model. The anomalous nature of the observation[11,12] of GMR in the absence of spontaneous magnetization in the insulating $n = 2$ Ruddlesden−Popper (RP) phases (Figure 1) $Sr_{2-x}Nd_{1+x}Mn_2O_7$ (x = 0.0, 0.1, 0.2) is particularly evident when the behavior of the Nd-containing phases is contrasted with that of the RP phase $Sr_{1.8}La_{1.2}Mn_2O_7$.[13] The latter compound shows a metal−insulator transition at its Curie temperature (126 K), and the GMR (-2×10^4% in 7 T) observed in this case can therefore be accounted for within the DE model. GMR is observed over a wide temperature range in $Sr_{2-x}Nd_{1+x}Mn_2O_7$, but only close to T_c in $Sr_{1.8}La_{1.2}Mn_2O_7$. However, this latter difference may well be due to the use of polycrystalline and single-crystal samples in the respective experiments.[14] These observations suggest that the behavior of these RP systems is very sensitive to the specific Ln element involved and to the relative concentration of Sr and Ln. In this paper we describe a study of $Sr_2LaMn_2O_7$ by high-resolution X-ray and neutron powder diffraction. We shall show that, as in the case of $Sr_{2-x}Nd_{1+x}Mn_2O_7$,[15,16] the crystal chemistry of this composition is very complex, with at least two structurally similar phases being present in the sample. The occurrence of this two-phase phenomenon in both $Sr_2LaMn_2O_7$ and $Sr_2NdMn_2O_7$, when considered in the

* To whom correspondence should be addressed.
† University of Oxford.
‡ Brookhaven National Laboratory.
§ Institut Laue-Langevin.
⊗ Abstract published in *Advance ACS Abstracts,* March 15, 1997.

(1) Urushibara, A.; Moritomo, Y.; Arima, T.; Asamitsu, A.; Kido, G.; Tokura, Y. *Phys. Rev. B* **1995**, *51*, 14103.
(2) Kusters, R. M.; Singleton, J.; Keen, D. A.; McGreevy, R.; Hayes, W. *Physica* **1989**, *B155*, 363.
(3) Zuotao, Z.; Yufang, R. *J. Solid State Chem.* **1996**, *121*, 138.
(4) Maignan, A.; Simon, C.; Caignaert, V.; Raveau, B. *J. Magn. Magn. Mater.* **1996**, *152*, L5.
(5) von Helmolt, R.; Wecker, J.; Lorenz, T.; Samwer, K. *Appl. Phys. Lett.* **1995**, *67*, 14.
(6) Zener, C. *Phys. Rev.* **1951**, *82*, 403.
(7) de Gennes, P. G. *Phys. Rev.* **1960**, *118*, 141.
(8) Cheong, S. W.; Hwang, H. Y.; Batlogg, B.; Rupp Jr., L. W. *Solid State Commun.* **1996**, *98*, 163.
(9) Shimakawa, Y. Kubo, Y.; Manako, T. *Nature* **1996**, *379*, 53.
(10) Subramanian, M. A.; Toby, B. H.; Ramirez, A. P.; Marshall, W. J.; Sleight, A. W.; Kwei, G. H. *Science* **1996**, *273*, 81.
(11) Battle, P. D.; Blundell, S. J.; Green, M. A.; Hayes, W.; Honold, M.; Klehe, A. K.; Laskey, N. S.; Millburn, J. E.; Murphy, L.; Rosseinsky, M. J.; Samarin, N. A.; Singleton, J.; Sluchanko, N. A.; Sullivan, S. P.; Vente, J. F. *J. Phys.: Condensed Matter* **1996**, *8*, L427.
(12) Seshadri, R.; Martin, C.; Maignan, A.; Hervieu, M.; Raveau, B.; Rao, C. N. R. *J. Mater. Chem.* **1996**, *6*, 1585.
(13) Moritomo, Y.; Asamitsu, A.; Kuwahara, H.; Tokura, Y. *Nature* **1996**, *380*, 141.
(14) Hwang, H. Y.; Cheong, S. W.; Ong, N. P.; Batlogg, B. *Phys. Rev. Lett.* **1996**, *77*, 2041.
(15) Battle, P. D.; Green, M. A.; Laskey, N. S.; Millburn, J. E.; Radaelli, P.; Rosseinsky, M. J.; Sullivan, S. P.; Vente, J. F. *Phys. Rev. B* **1996**, *54*, 15967.
(16) Battle, P. D.; Green, M. A.; Laskey, N. S.; Millburn, J. E.; Murphy, L.; Rosseinsky, M. J.; Sullivan, S. P.; Vente, J. F. *Chem. Mater.*, in press.

S0897-4756(96)00632-1 CCC: $14.00

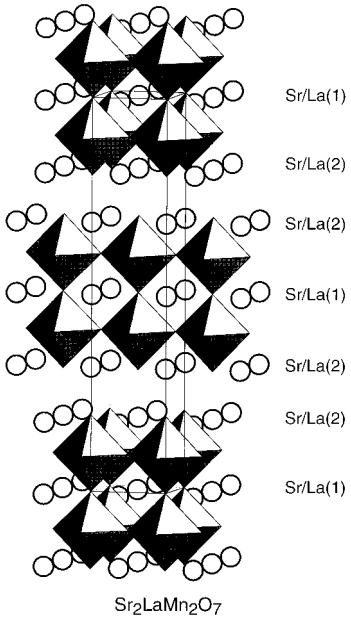

Figure 1. $n = 2$ Ruddlesden−Popper crystal structure of $Sr_2LaMn_2O_7$. MnO_6 octahedra are shaded and the Sr/La sites are shown as circles.

light of the knowledge that $Sr_{1.8}La_{1.2}Mn_2O_7$[13] and $Sr_{1.6}Nd_{1.4}Mn_2O_7$[16] can be prepared as single phases, leads us to suggest that the $n = 2$ RP structure is inherently unstable for Ln = La, Nd when the mean oxidation state of Mn is close to 3.5. Some perovskites (i.e. $n = \infty$ RP phases)[17−19] and K_2NiF_4 phases (i.e., $n =$ 1 RP)[20−22] show charge-ordering phenomena at this oxidation state, an option which is apparently not open to the $n = 2$ La and Nd phases. Despite the similarity of their structural behavior, the magnetic properties of $Sr_2LnMn_2O_7$ (Ln = La or Nd) differ markedly over a wide temperature range.[11,23] For example, whereas the Nd samples consist of a spin glass and an antiferromagnetic component at 1.7 K, the sample of $Sr_2LaMn_2O_7$ described below contains antiferromagnetic and ferromagnetic components, and thus serves to illustrate the dependence of the electronic properties on both the atomic number of Ln and, by comparison with $Sr_{1.8}La_{1.2}Mn_2O_7$, on the Sr/Ln ratio.

Experimental Section

The preparation of the sample of $Sr_2LaMn_2O_7$ used in this study and its preliminary structural characterization by X-ray powder diffraction have been described previously.[11,16,23] The synthesis involved firing stoichiometric quantities of dry La_2O_3, MnO_2, and $SrCO_3$ in an alumina boat in air at 800 °C for 12 h, 1000 °C for 24 h, and 1200 °C for 24 h, and then regrinding, pelletizing, and firing for 4 days at 1400 °C with one further regrind. The product was furnace-cooled to 1100 °C and then air-quenched. Volumetric analysis has subsequently established the mean oxidation state of Mn as 3.506(3). Neutron powder diffraction patterns were collected at 1.7 K on the diffractometer D2b ($5 \leq 2\theta/\text{deg} \leq 150$, $\Delta 2\theta = 0.05°$) at the Institut Laue Langevin, Grenoble.[24,25] Data were collected at two different wavelengths, 1.594 12 and 2.3979 Å, on a sample contained in a cylindrical vanadium can of diameter 8 mm. A 20′ α_2 collimator was inserted in the primary beam in order to enhance the low-angle resolution. The diffraction patterns were analyzed by the Rietveld technique[26] using the program package GSAS.[27] The following neutron scattering lengths were used: $b_{Sr} = 0.702$, $b_{La} = 0.827$, $b_{Mn} = -0.373$, and $b_O = 0.5805 \times 10^{-14}$ m. The free ion form factor of Mn^{3+} [28] was used to describe the angular dependence of the magnetic scattering amplitude. Data were also collected in the temperature range $110 \leq T/\text{K} \leq 230$ using the lower resolution powder diffractometer D1b (mean wavelength 2.520 Å, $5 \leq 2\theta/° \leq 85$). During the course of this experiment the sample temperature was increased at a rate of ~15 K h^{-1}, and the data from the position- sensitive detector were stored every 10 min, thus producing a set of diffraction patterns with a temperature resolution of ~2.5 K. These data were subsequently analyzed in order to define the temperature dependence of the ordered magnetic moment.

Synchrotron X-ray data were collected at beamline X7A at the Brookhaven National Synchrotron Light Source. The sample was pressed on to a flat Cu plate which had been lightly smeared with Vaseline, and loaded into a Displex closed-cycle He cryostat. A wavelength of 0.7799 Å was selected from a channel-cut double-crystal Ge (111) monochromator, and a Ge (220) crystal analyzer was mounted in the diffracted beam. Step scans were carried out at 300 and 20 K ($4 \leq 2\theta/\text{deg} \leq 31$, $\Delta 2\theta = 0.01°$). The sample was rocked over a narrow angular range to ensure proper powder averaging. The temperature dependence of the lattice parameters was investigated by analyzing the positions of the {105} and {110} reflections as a function of temperature.

Results

Analysis of the X-ray diffraction data recorded on $Sr_2LaMn_2O_7$ using the synchrotron source showed that the full structural complexity of this sample was not revealed in our previous laboratory-based study.[23] The diffraction patterns recorded at 300 and 20 K both showed the presence of at least two tetragonal RP $n = 2$ phases with closely related lattice parameters; at 300 K, $a = 3.8748(1)$ Å, $c = 19.9984(8)$ Å for the majority phase, and $a = 3.8753(3)$ Å, $c = 20.072(1)$ Å for the minority component (~25%). The asymmetric profile of the {0 0 10} reflection (Figure 2) showed that additional inhomogeneities were present, but there was no evidence for the presence of impurities such as $(Sr/La)MnO_3$ or $(Sr/La)_2MnO_4$. The temperature dependence of c/a for the majority phase, obtained by fitting the profiles of the {105} and {110} reflections to two peaks of the same shape and width, is shown in Figure 3. The data are clearly nonlinear, with little variation apparent below 100 K; there is some suggestion of a discontinuity at ~200 K. The variation in the value of c/a above 100 K demonstrates that the thermal contraction in this phase is anisotropic, and comparison of the values $c_{20\text{ K}}/c_{300\text{ K}} = 0.994\,98$ and $a_{20\text{ K}}/a_{300\text{ K}} = 0.999\,46$ shows that the contraction is most pronounced

(17) Tomioka, Y.; Asamitsu, A.; Moritomo, Y.; Kuwahara, K.; Tokura, Y. *Phys. Rev. Lett.* **1995**, *74*, 5108.
(18) Tomioka, Y.; Asamitsu, A.; Kuwahara, H.; Moritomo, Y.; Tokura, Y. *Phys. Rev. B* **1996**, *53*, R1689.
(19) Lees, M. R.; Barratt, J.; Balakrishnan, G.; Paul, D. M. *Phys. Rev. B* **1995**, *52*, R14303.
(20) Bouloux, J. C.; Soubeyroux, J. L.; Daoudi, A.; Flem, G. L. *Mater. Res. Bull.* **1981**, *16*, 855.
(21) Bao, W.; Chen, C. H.; Carter, S. A.; Cheong, S.-W. *Solid State Commun.* **1996**, *98*, 55.
(22) Moritomo, Y.; Tomioka, Y.; Asamitsu, A.; Tokura, Y. *Phys Rev. B* **1995**, *51*, 3297.
(23) Battle, P. D.; Green, M. A.; Laskey, N. S.; Millburn, J. E.; Rosseinsky, M. J.; Sullivan, S. P.; Vente, J. F. *Chem. Commun.* **1996**, 767.
(24) Pannetier, J.; *Chem. Scr.* **1986**, *26A*, 131.
(25) Hewat, A. W. *Mater. Sci. Forum* **1986**, *9*, 69.
(26) Rietveld, H. M. *J. Appl. Crystallogr.* **1969**, *2*, 65.
(27) Larson, A. C.; von Dreele, R. B. General Structure Analysis System (GSAS), Los Alamos National Laboratories, Report LAUR 86-748, 1990.
(28) Watson, R. E.; Freeman, A. J. *Acta Crystallogr.* **1961**, *14*, 27.

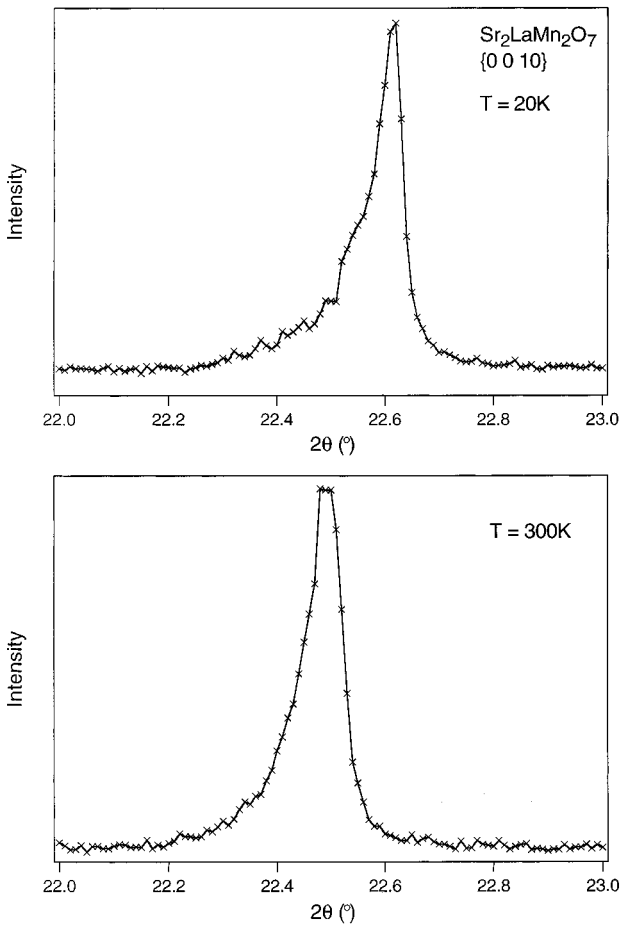

Figure 2. Synchrotron X-ray powder diffraction profile of the {0 0 10} reflection of $Sr_2LaMn_2O_7$ at 20 and 300 K.

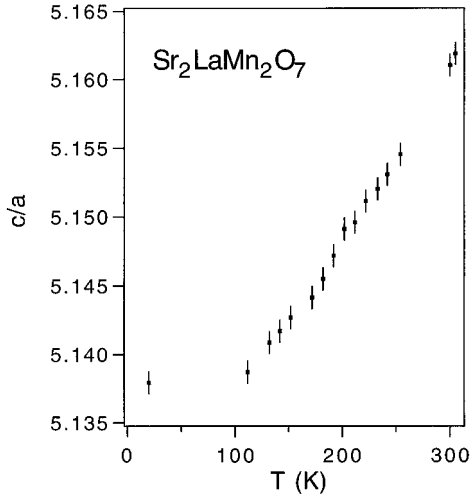

Figure 3. Dependence of *c*/*a* on temperature for the majority phase in $Sr_2LaMn_2O_7$. Estimated errors in *a* and *c* are 0.0002 and 0.003 Å, respectively, based on an error in peak position of 0.001°.

in the direction perpendicular to the perovskite layers. The increased scatter on the peak positions derived for the minority phase prohibited detailed analysis in that case.

The multiphasic nature of the sample was also apparent in the neutron data collected on D2b at 1.7 K. In addition to the Bragg peaks characteristic of the crystal structure, the latter data set contained purely magnetic Bragg peaks. A reasonable level of agreement between the observed and calculated neutron diffraction

Table 1. Generalized Crystallography for the $n = 2$ Ruddlesden−Popper Structure, Space Group *I4/mmm*

atom	site	coordinates
Sr/Ln(1)	2b	0 0 $^1/_2$
Sr/Ln(2)	4e	0 0 *z*; $z \sim 0.7$
Mn	4e	0 0 *z*; $z \sim 0.1$
O(1)	2a	0 0 0
O(2)	4e	0 0 *z*; $z \sim 0.2$
O(3)	8g	0 $^1/_2$ *z*; $z \sim 0.1$

patterns was achieved by applying a biphasic model. The choice of the parameter set to be used in this structure refinement was not straightforward because, although the profiles of the Bragg peaks showed that at least two phases were present in the sample, the resolution of D2b was insufficient to separate the contributions from the different phases. This failure is hardly surprising in view of the remarkable structural similarity between the two phases, but it did lead to strong correlations between parameters in the least-squares analysis. It became clear that it would be impossible to achieve a stable refinement using the ideal, full parameter set, and constraints were therefore applied to the overall profile parameters. Two suitable sets of constraints were identified after preliminary refinements and the data were then analyzed independently using both sets. There were no chemically or magnetically significant differences between the two final, refined structural models, and we therefore believe that the conclusions we draw below are robust against reasonable changes in the data analysis strategy. Both the refinements involved simultaneous analysis of data collected using $\lambda \sim 1.59$ and $\lambda \sim 2.39$ Å. The results described below are those from one of the two independent approaches in which the majority phase (phase 1) was finally modeled using five peak-shape parameters (GU, GV, GW, LY, ASYM[27]) for both wavelengths and the minority phase (phase 2) by 3 (GU, GW, ASYM) at 1.59 Å and by 4 (GU, GV, GW, ASYM) at 2.39 Å. The relative concentration of the two phases was allowed to vary. The background level in the 1.59 Å (2.39 Å) data was modeled using a 12 (6) term shifted Chebychev polynomial. All atomic parameters were allowed to vary independently in the two phases with the exception of the isotropic temperature factor of each crystallographic site, which was constrained to be the same in both. The compositions of the two phases present in the sample of overall composition $Sr_2LaMn_2O_7$ were too similar to be distinguished, particularly in view of the similarity between the neutron scattering lengths of Sr and La. This similarity also necessitated the assumption that the Sr and La cations are disordered over the two available crystallographic sites (Table 1), one in the center of the perovskite block (Sr/Ln(1) at (001/2)) and the other in the rock-salt layer of the RP structure (Sr/Ln(2) at (00*z*), $z \sim 0.7$).

Inspection of the diffraction pattern showed that the distribution of magnetic scattering was very similar to that previously observed from $Sr_2NdMn_2O_7$[15] in the temperature range $30 \leq T/K \leq 130$. The reflections of magnetic origin could all be indexed using the chemical unit cell, but the presence of {00*l*} reflections with $l = 2n + 1$ indicated first that the magnetic structure which gives rise to these peaks is not body centered and second that the magnetic moments do not align parallel to the *z* axis. Consequently, the antiferromagnetic structure shown in Figure 4 was taken as a trial model. In this

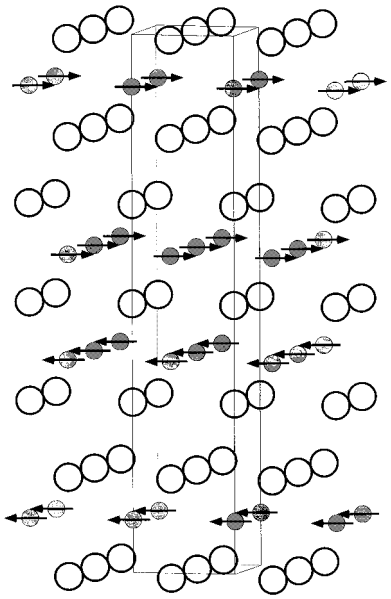

Figure 4. Magnetic structure of the antiferromagnetic phase in $Sr_2LaMn_2O_7$. Mn sites are shaded and the Sr/La atoms are shown as unshaded circles. Arrows indicate the direction of the magnetic moments.

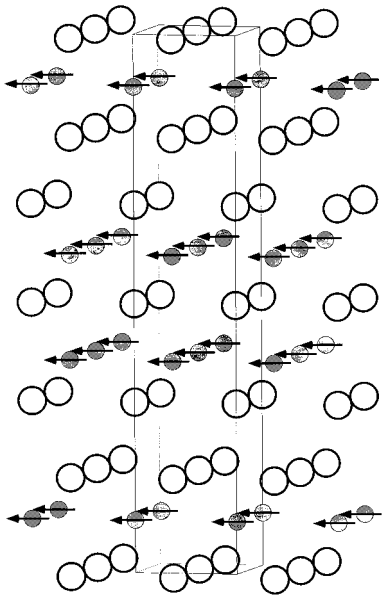

Figure 5. Magnetic structure of the ferromagnetic phase in $Sr_2LaMn_2O_7$. Mn sites are shaded and the Sr/La atoms are shown as unshaded circles. Arrows indicate the direction of the magnetic moments.

model the Mn moments are constrained to lie in the *xy* plane, thus lowering the magnetic symmetry to orthorhombic. It was concluded, following an initial analysis in which the unit cell parameters of the antiferromagnetic structure were not tied to either structural phase, that only the majority phase shows this antiferromagnetic ordering. The ordered moment was found to be 2.88(1) μ_B per Mn; when the constraint on the direction of the moment was lifted, the *z* component refined to zero. Careful examination of the difference profile at this stage showed that there was some feeble intensity left unaccounted for in the reflections $\{00l\}$ with $l = 2n$. This could be modeled with a ferromagnetic structure in which the magnetic moments of Mn were again aligned in the *xy* plane (Figure 5). The angular positions of these reflections suggested that they arose from the minority phase rather than from the majority phase and this was confirmed by Rietveld refinement of the possible models (Figure 6). Assignment of the ferromagnetism to the minority phase resulted in an ordered moment of 2.16(8) μ_B per Mn. In the final cycles of refinement a total of 60 parameters were present, resulting in an agreement factor R_{wp} of 7.85%. The atomic parameters derived from this two-phase refinement of the structure of $Sr_2LaMn_2O_7$ and the resultant bond distances and angles are given in Tables 2 and 3. Figure 7 shows the final observed and calculated diffraction patterns. We attempted to account for the remaining features in the difference plot by lowering the symmetry of the majority phase in a way that permitted the displacement of the oxide ions that would be expected to accompany charge ordering on the Mn sublattice. However, the angular distribution of the additional calculated intensity did not correspond to that observed, and we shall therefore assume in the discussion below that charge ordering does not occur in this system. Our second refinement strategy, which was mentioned above but not described in detail, employed a different choice of constraints on the peak profile parameters and resulted in magnetic moments of 2.98(2)

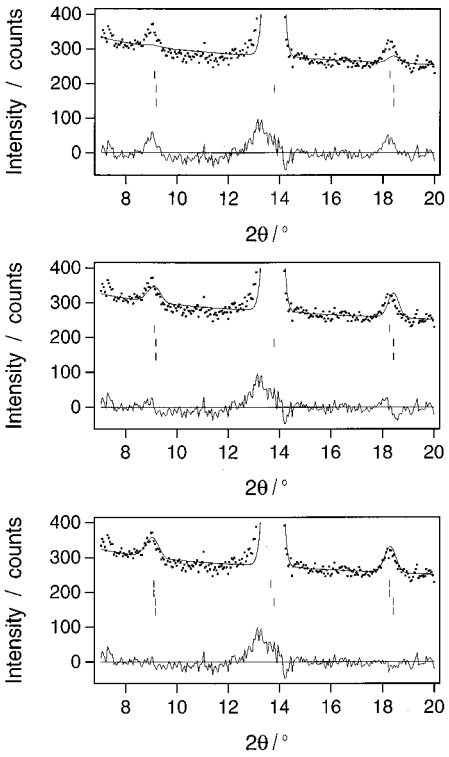

Figure 6. Detail of the neutron diffraction profile ($\lambda = 1.59$ Å) of $Sr_2LaMn_2O_7$ modeled as (a, top) AFM only (b, middle) both AFM and FM ordering in majority phase (c, bottom) AFM ordering in phase 1 and FM ordering in phase 2.

and 2.14(7) μ_B for the Mn cations in the antiferromagnetic and ferromagnetic phases respectively, with a phase distribution of 75(1):25(1)%. The difference between these values and those listed in Table 2 gives an indication of the sensitivity of our results to the choice of parameter set.

The development of the neutron diffraction pattern of $Sr_2LaMn_2O_7$ as a function of temperature in the range $110 \leq T/K \leq 220$ was studied using data collected on D1b. The additional magnetic intensity in the peaks

Table 2. Crystallographic Data for $Sr_2LaMn_2O_7$ at 1.7 K

	phase 1	phase 2
a (Å)	3.87419(7)	3.8664(2)
c (Å)	19.9059(4)	20.038(2)
V (Å^3)	298.77(2)	299.56(3)
fraction (%)	81(1)	19(1)
U_{iso} (Sr/La1) (Å^2)	0.0003(5)	
z (Sr/La2)	0.68211(7)	0.6841(4)
U_{iso} (Sr/La2) (Å^2)	0.0021(3)	
z (Mn)	0.0966(1)	0.0968(6)
U_{iso} (Mn) (Å^2)	−0.0004(4)	
U_{iso} (O1) (Å^2)	0.0042(5)	
z (O2)	0.1949(1)	0.1935(5)
U_{iso} (O2) (Å^2)	0.0066(5)	
z (O3)	0.09467(8)	0.0947(3)
U_{iso} (O3) (Å^2)	0.0046(2)	
μ_{AFM} (μB)	2.88(1)	
μ_{FM} (μB)		2.16(8)
R_{wp}, R_p 1.6 Å (%)	6.99	5.28
R_{wp}, R_p 2.4 Å (%)	9.35	6.74
R_{wp}, R_p overall (%)	7.86	5.53
χ_{red}^2, DWd	5.77	0.33

Table 3. Bond Lengths (Å) and Selected Bond Angles (deg) in $Sr_2LaMn_2O_7$ at 1.7 K

	phase 1	phase 2
Mn−O(1) (1×)	1.923(3)	1.94(1)
Mn−O(2) (1×)	1.957(4)	1.94(2)
Mn−O(3) (4×)	1.9375(1)	1.9336(3)
Mn−Mn (z,−z)	3.846(6)	3.88(3)
Sr/La(1)−O(1) (4×)	2.7395(1)	2.7340(1)
Sr/La(1)−O(3) (8×)	2.703(1)	2.710(5)
Sr/La(2)−O(2) (1×)	2.448(3)	2.45(1)
Sr/La(2)−O(2) (4×)	2.7513(2)	2.7405(9)
Sr/La(2)−O(3) (4×)	2.604(2)	2.635(8)
O(1)−Mn−O(3)	88.9(1)	88.8(5)
O(3)−Mn−O(3)	177.7(3)	177.6(9)

which contain a nuclear scattering contribution is lost in the experimental noise above 124 ± 2 K, while the purely magnetic Bragg reflections are visible below 211 ± 2 K (Figure 8). The evolution of the magnetic structure of $Sr_2LaMn_2O_7$ with temperature was quantified by analyzing the individual diffraction patterns. The atomic coordinates and the phase fractions were held constant during the course of these refinements, which were concerned primarily with the magnitude of the ordered atomic magnetic moments. Their outcome is summarized in Figure 9.

Discussion

The behavior of our sample of overall composition $Sr_2LaMn_2O_7$ is clearly very complex. The results described above suggest that it is best explained by considering the sample to be a biphasic mixture. However, this approach raises a number of questions, the most obvious of which concerns our synthesis. The fact that we have successfully prepared[16] monophasic samples of $Sr_2LnMn_2O_7$ for Ln = Tb, Dy, Ho, Er, and Y suggests that our preparative method is not grossly flawed, and yet we have been unable to prepare single phase samples of this stoichiometry for Ln = La, Nd, Pr, Sm, and Gd. The unit cell parameters of the components of the biphasic samples are so similar that it is all too easy to interpret X-ray powder diffraction data collected on a laboratory-based diffractometer by assuming, incorrectly, that only one phase is present; we now accept that we made this mistake in our initial analysis of $Sr_2LaMn_2O_7$,[23] despite the fact that a monophasic Rietveld analysis of our X-ray data resulted

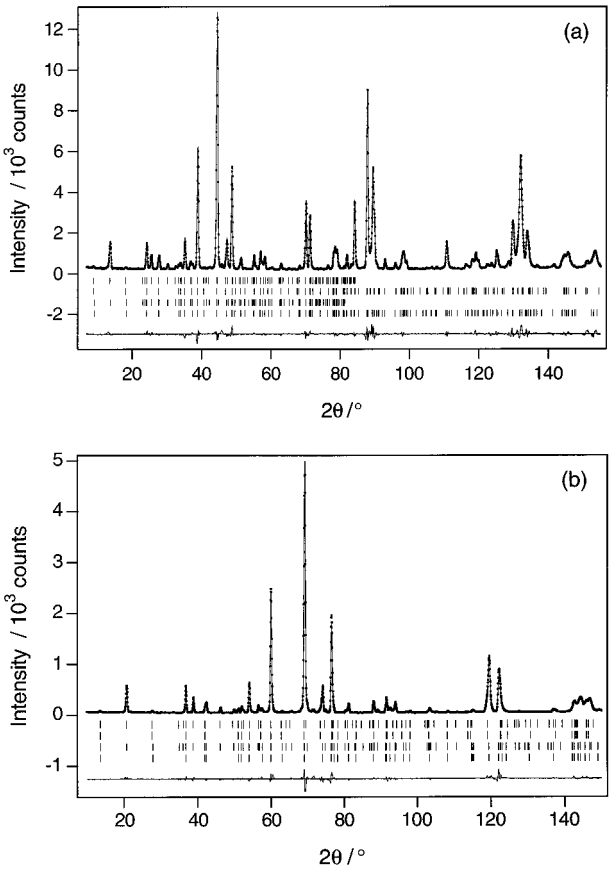

Figure 7. Observed, calculated, and difference neutron powder diffraction patterns for $Sr_2LaMn_2O_7$ at 1.7 K: (a) $\lambda \sim 1.59$ Å, (b) $\lambda \sim 2.39$ Å. Reflection positions are marked for both phase 1 (lower) and phase 2 (upper) as well as for the allowed magnetic reflections with are given above the nuclear reflections.

in a value of R_{wpr} as low as 9.24%. We have therefore begun to question earlier reports of the synthesis of single-phase $Sr_2LaMn_2O_7$. The saturation magnetic moments of the samples prepared at 1400 °C by MacChesney et al.[29] and at 1230−1330 °C by Mohan Ram et al.[30] ($M_{sat} = 0.25\mu_B$ and $0.5\mu_B$ per Mn, respectively) are similar to that of our own (1400 °C) sample ($M_{sat} = 0.35\mu_B$ per Mn)[23] and we take this as evidence to suggest that their samples were similar in nature to our own. It is interesting to note that MacChesney et al. were sufficiently puzzled by their magnetic data that they questioned the phase-purity of their sample. We now believe that the composition $Sr_2LaMn_2O_7$ cannot be prepared by a high-temperature route and that the samples described previously by other groups were also biphasic. This then raises the possibility that whereas other RP phases containing Mn in an average oxidation state close to 3.5 show charge ordering effects over a composition range which depends on n and the elemental composition,[17−22] the $n = 2$ RP phases containing the larger lanthanides are, for some reason, unable to stabilize in this way and they consequently disproprotionate.

The above discussion leads us to question the assumption, made in our data analysis, that the two

(29) MacChesney, J. B.; Potter, J. F.; Sherwood, R. C. *J. Appl. Phys.* **1969**, *40*, 1243.
(30) Mohan-Ram, R. A.; Ganguly, P.; Rao, C. N. R. *J. Solid State Chem.* **1987**, *70*, 82.

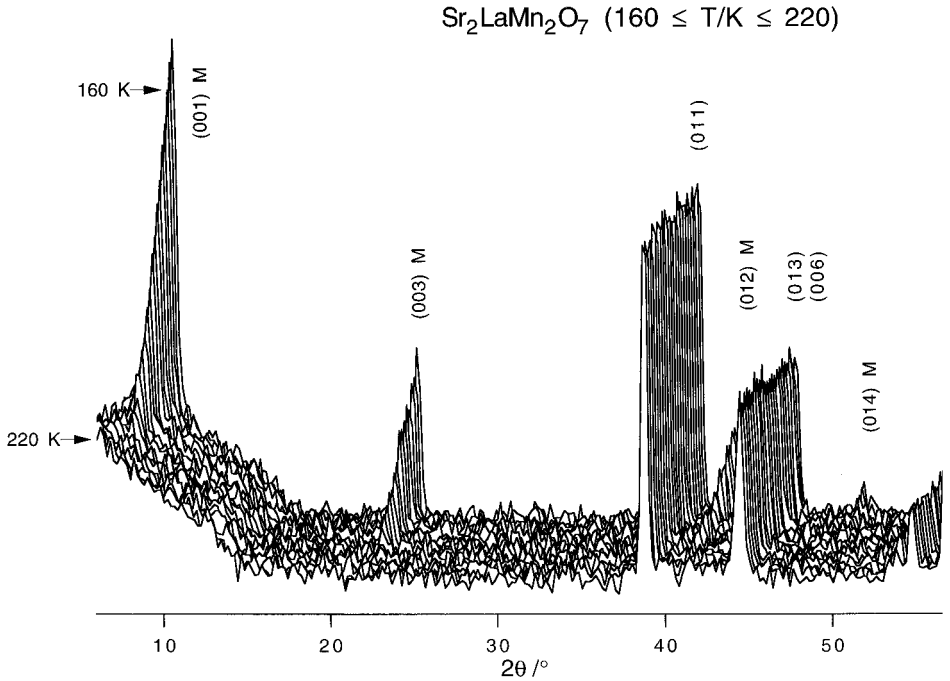

Figure 8. Development of the neutron diffraction pattern for $Sr_2LaMn_2O_7$ as a function of the temperature in the angular range $5 \leq 2\theta/\text{deg} \leq 55$ ($\lambda \sim 2.5$ Å). The Bragg reflections are indexed and the magnetic peaks are marked.

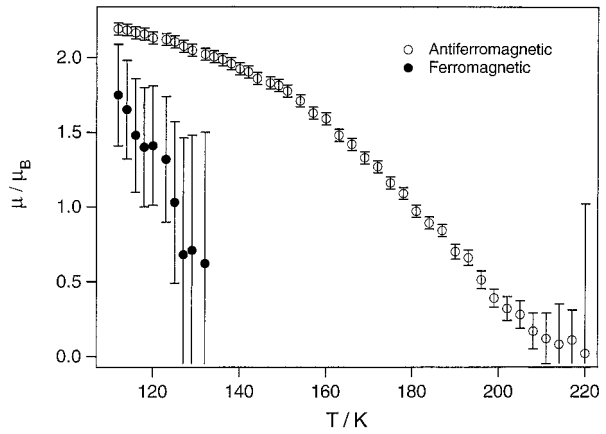

Figure 9. Average ordered magnetic moment per Mn in $Sr_2LaMn_2O_7$ as a function of temperature; open circles represent the AFM term in phase 1 and filled circles give the FM term in phase 2.

components in our sample have the same elemental composition. The data in Table 2 show that the unit cell volume of phase 1 is 0.26% less than that of phase 2, a difference which is large enough to suggest that the two phases have different compositions. Simultaneous consideration of our neutron and magnetization data leads us to suggest that our sample consists of a small amount (19%) of a phase which is ferromagnetic below ~120 K, and a larger amount of a phase which is antiferromagnetic below ~211 K. (This is the first conclusive evidence for the presence of an antiferromagnetic phase in the $Sr_2LaMn_2O_7$ system.) In view of the high value of $\delta T_c/\delta x$ found in these systems,[1] phase 2 must have a composition very close to $Sr_{1.8}La_{1.2}Mn_2O_7$, single crystals of which have been shown to order ferromagnetically, with the spins in the *xy* plane, at 126 K.[13] If this assignment is correct, then the overall composition of our sample, confirmed by the results of our volumetric analysis, dictates that phase 1 has the stoichiometry $Sr_{2.04}La_{0.96}Mn_2O_7$. The unit cell parameters determined[31] for a sample of nominal composition $Sr_{1.8}La_{1.2}Mn_2O_7$ at 20 K are $a = 3.8675$, $c = 20.061$ Å, in reasonable agreement with those reported for phase 2 in Table 2, although the sample used in the determination of these values was contaminated with ~10% of an $n = 1$ RP phase and its stoichiometry may therefore not be accurate. The value of the ordered magnetic moment in phase 2 is lower than that ($3.0\mu_B$) determined in a neutron study[31] of $Sr_{1.8}La_{1.2}Mn_2O_7$, and also lower than the value of the saturation magnetization measured in 5 T by Moritomo et al.[13] Our refined value is in good agreement with the saturation value measured in a field of 0.05 T by Seshadri et al.[12] The manner in which the magnetization of different samples reaches a field-dependent saturation value at $\sim 0.9T_c$ in any applied field $H \geq 0.001$ T[12,13] suggests that small magnetic domains are relatively stable in this material and that the relatively low value of the moment determined for phase 2 in our neutron measurement may be due in part to a failure of the assumption, implicit in magnetic powder diffraction, that the magnetic domains in a powder sample are all larger than the coherence length of the neutron beam. The low-temperature ordered magnetic moment of the Mn cations in phase 1 is closer to the expected value ($gS = 3.5\mu_B$) and is comparable to that measured in the antiferromagnetic phase of $Sr_2NdMn_2O_7$. It should be noted that the magnitude of the magnetic moments is sensitive to the choice of form factor and that they are also strongly correlated with the phase fractions in the least-squares calculations. In view of the uncertainties outlined above, we are cautious about assigning specific stoichiometries to the phases in our sample on the basis of the magnetic data. We are, however, confident that the interpretation of our data in terms of a La-rich ferromagnetic phase and a Sr-rich antiferromagnetic phase is correct. It is unfortunate that the difference

(31) Mitchell, J. F.; Argyriou, D. N.; Jorgensen, J. D.; Hinks, D. G.; Potter, C. P.; Bader, S. D. *Phys. Rev. B.* **1997**, *55*, 63.

in the neutron scattering lengths of Sr and La is insufficient to permit this to be confirmed directly from the diffraction data.

The bond lengths listed in Table 3 show that there is no significant difference in size between the Sr/La(1) site in phase 1 and that in phase 2; the same is true of the Sr/La(2) sites. These data thus provide no evidence for the presence of different Sr/La distributions in the two phases. In each case the Sr/La(1) site is larger than the Sr/La(2) site, as is to be expected in view of the larger coordination number. Again the neutron data failed to reveal any departure from a statistical distribution of Sr and La over the two sites in either phase, although evidence from X-ray diffraction[12,16] suggests that La preferentially occupies the 12 coordinate Sr/La(1) site. This partial ordering must be driven by considerations of charge rather than size. More interesting conclusions can be drawn from the neutron data by considering the environment of the Mn cations. The distance between the transition metal ions at (00z) and (00$-z$) is significantly shorter in antiferromagnetic phase 1 than it is in ferromagnetic phase 2. It is also shorter than the corresponding distance (3.872(4) Å)[31] in $Sr_{1.8}La_{1.2}Mn_2O_7$, the latter distance being close to the value refined for phase 2 in our sample. Similarly, the Mn−O distance within the layers (Mn−O(3)) in phase 1 is significantly longer than that in phase 2, the latter being similar to that found in $Sr_{1.8}La_{1.2}Mn_2O_7$. It should be borne in mind that this last point follows from the comparison of unit cell parameters made earlier. It is thus clear that the magnetic differences between phase 1 and phase 2 are matched by structural differences and that aspects of the crystal structure reinforce the comparisons between phase 2 and $Sr_{1.8}La_{1.2}Mn_2O_7$ which were made on basis of the magnetic data. Finally, it is interesting to compare the mean metal−oxygen bond length and its variance in a number of compounds. The mean (variance) distances for $La_{0.5}Ca_{0.5}MnO_3$ above the charge ordering temperature (T_{co}), $La_{0.5}Ca_{0.5}MnO_3$ below T_{co}, phase 1, and $Sr_3Ti_2O_7$[32] are 1.944 (0.002), 1.943 (0.020), 1.939 (0.010), and 1.958 (0.009) Å, respectively; the spread of the distances is thus greater in the charge-ordered $n = \infty$ phase $La_{0.5}Ca_{0.5}MnO_3$ than in either of the $n = 2$ phases, despite the inherently anisotropic environment in the latter. This observation supports the conclusion, drawn from our Rietveld analysis, that phase 1 does not show charge ordering.

The variation in the bond lengths between phase 1 and phase 2, and the change from antiferromagnetism to ferromagnetism, may arise from variations in the occupancy of the cation d bands in two phases which contain Mn in different mean oxidation states (Mn +3.4 in $Sr_{1.8}La_{1.2}Mn_2O_7$, Mn +3.52 in $Sr_{2.04}La_{0.96}Mn_2O_7$); a reduction in the number of e_g electrons leads to a weakening of the ferromagnetic interaction. This is a very different explanation from that used in the case of biphasic $Sr_2NdMn_2O_7$, where the difference in unit cell volume between the two phases was insignificant (0.03%) and we concluded that there was no variation in composition through the sample but that the Sr/Nd ordering over the two available sites was subtly different in the two phases. This assumption enabled us to explain the occurrence of an antiferromagnetic phase and a spin glass phase. The absence of any difference in the size of the Sr/La sites between the two phases of $Sr_2LaMn_2O_7$ prevents us from using this argument again. The change in behavior might relate to some extent to the different influence of diamagnetic La compared to paramagnetic Nd, but this is unlikely to have a significant effect on phase transitions which take place at $T > 100$ K. We thus believe that we are dealing with a biphasic sample which demonstrates the dramatic changes in physical properties that can occur as a result of small changes in chemical composition. The behavior of this system should act as a warning to those, including ourselves, who rely on laboratory-based diffractometers to establish phase purity. We have now begun a program of electron microscopy which will enable us to characterize our sample over shorter length scales. There is also a need for a careful synthetic study to establish the phase diagram of the system.

Data on the GMR manganites are being accumulated at a remarkable rate, and it is instructive to consider how the results described above fit into the emerging experimental picture. It appears that several electronic ground states are possible in Mn^{III}/Mn^{IV} oxides and that the size of the lanthanide and alkaline earth cations, the Mn oxidation state, and the number of contiguous layers of corner-sharing MnO_6 octahedra all influence which ground state is adopted for a particular compound. At the nominal Mn +3.5 oxidation state, $La_{0.5}Sr_{0.5}MnO_3$ ($n = \infty$) is metallic in both paramagnetic and ferromagnetic states,[1] with no indication of the charge ordering instability found for $La_{0.5}Ca_{0.5}MnO_3$.[33] However, the $n = 1$ phase $La_{0.5}Sr_{1.5}MnO_4$ undergoes charge-ordering at 217 K, forming a $\sqrt{2}a \times \sqrt{2}a \times c$ unit cell, followed by antiferromagnetic ordering at 117 K.[34] The behavior of $La_{0.5}Ca_{0.5}MnO_3$ is particularly complex, with ferromagnetic ordering at 225 K and antiferromagnetic order below 155 K. High-resolution powder diffraction studies[35] have shown that, between these two temperatures, a range of partially Jahn−Teller ordered, metastable phases coexist in the sample. Of the two phases which form the core of the present study, $Sr_{1.8}La_{1.2}Mn_2O_7$ has already been shown to be a ferromagnetic metal below a Curie temperature of 126 K (comparable to the Néel temperature of $Sr_2NdMn_2O_7$ and $Sr_{1.9}Nd_{1.1}Mn_2O_7$). The new, Sr-rich phase which we have characterized here is an antiferromagnet (this is consistent with the phase being an insulator) with a Mn oxidation state slightly greater than +3.5 (an increase which may be enough to suppress commensurate charge ordering) and a remarkably high 3D Néel temperature of 211 K. The observation of antiferromagnetism with oxidation states in excess of +3.5 is consistent with the behavior of $La_{1-x}Ca_xMnO_3$ but not with that of $La_{1-x}Sr_xMnO_3$, which remains ferromagnetic due presumably to the direct exchange interaction which is mediated by the itinerant σ^* electrons; the antiferromagnetic $t_{2g}-t_{2g}$ superexchange dominates when the concentration of σ^* carriers is sufficiently reduced.

(32) Elcombe, M. M.; Kisi, E. H.; Hawkins, K. D.; White, T. J.; Goodman, P.; Matheson, S. *Acta Crystallogr.* **1991**, *B47*, 305.

(33) Ramirez, A. P.; Schiffer, P.; Cheong, S. W.; Chen, C. H.; Bao, W.; Palstra, T. T. M.; Gammel, P. L.; Bishop, D. J.; Zegarski, B. *Phys. Rev. Lett.* **1996**, *76*, 3188.

(34) Sternlieb, B. J.; Hill, J. P.; Wildgruber, U. C.; Luke, G. M.; Nachumi, B.; Moritomo, Y.; Tokura, Y. *Phys. Rev. Lett.* **1996**, *76*, 2169.

(35) Radaelli, P. G.; Cox, D. E.; Marezio, M.; Cheong, S. W. *Phys. Rev. B*, to be published.

The ferromagnetic interactions seem to compete less strongly in $Sr_{2.04}La_{0.96}Mn_2O_7$ than in $La_{0.5}Ca_{0.5}MnO_3$ which shows both types of order. The electronic properties of the structural family $(La,Sr)_{n+1}Mn_nO_{3n+1}$ can be linked to the dimensionality of the crystal structure by the following argument. Antiferromagnetic interactions dominate in the $n = 1$ (K_2NiF_4) phases,[34] indicating that double exchange is not a strong effect here, an observation that is consistent with the presence of localized electrons. The $n = \infty$ perovskites show ferromagnetism and metallic conductivity over a wide range of Mn oxidation states,[1] suggesting that double exchange is dominant among itinerant e_g electrons. Our data show that in the $n = 2$ case, with perovskite blocks (and hence e_g bands) of intermediate width, the balance between antiferromagnetism and ferromagnetism is very sensitive to the Mn oxidation state and that neither magnetic ground state is stable over the wide composition range associated with ferromagnetism in $n = \infty$ and antiferromagnetic interactions in $n = 1$. There may be a link between the electronic properties and the separation into two phases, which we believe has occurred in samples of $Sr_2LaMn_2O_7$ prepared by other workers as well as in our own.

Acknowledgment. We are grateful to the EPSRC and the donors of the Petroleum Research Fund, administered by the American Chemical Society, for financial support. Work at Brookhaven is supported under Contract No. DE-AC02-76CH00016, Division of Materials Sciences, U.S. Department of Energy. Chemical analyses were performed by N. Kasmir. The Argonne group kindly made a preprint of their work available to us.

CM960632D